Kuramoto model with run-and-tumble dynamics

Derek Frydel
Department of Chemistry, Universidad Técnica Federico Santa María, Campus San Joaquin, Santiago, Chile

(Received 18 May 2021; accepted 16 July 2021; published 4 August 2021)

This work considers an extension of the Kuramoto model with run-and-tumble dynamics—a type of self-propelled motion. The difference between the extended and the original model is that in the extended version angular velocity of individual particles is no longer fixed but can change sporadically with a new velocity drawn from a distribution $g(\omega)$. Because the Kuramoto model undergoes phase transition, it offers a simple case study for investigating phase transition for a system with self-propelled particles.

DOI: 10.1103/PhysRevE.104.024203

I. INTRODUCTION

This work considers an extension of the Kuramoto model that incorporates self-propelled dynamics. Originally conceived as a model of synchronization [1–6], the Kuramoto model consists of particles moving on a circle with angular velocities distributed according to $g(\omega)$. Even if particles move incoherently, due to coupling interactions, the system transitions to a coherent state, in which a fraction of particles locks onto the same angular velocity. The critical value of a coupling constant where the transition transpires can be calculated exactly using linear analysis [3].

Self-propelled dynamics is incorporated into the Kuramoto model by introducing a linear "reaction" term into the Fokker-Planck (FP) equation. Without the reaction term, an angular velocity of a given particle does not change in time. The source of disorder comes from the fact that different particles have different velocities in accordance with some distribution $g(\omega)$. This creates a dynamic quenched disorder [7]. With the reaction term, angular velocity of individual particles changes in the course of time by sampling the distribution $g(\omega)$. At the microscopic level, this means that individual particles change velocity at intervals drawn from a Poisson distribution. Then a new velocity is drawn from the distribution $g(\omega)$.

The proposed extension of the Kuramoto model is closely related to a model of self-propelled particles known as the run-and-tumble particles (RTP) [8]. In this model, particles are subject to a drift of constant velocity but changing orientation. In one dimension, where only two orientations are possible, the model can be solved exactly for particles confined between two walls [8–18]. Particles in this model are ideal, that is, noninteracting, and so there can be no phase transition yet, despite its simplicity, the model accurately captures many features of self-propelled motion. For example, it captures the deposition of particles in a steady state near the confining walls [19–23], a feature that is not accounted for by a Boltzmann distribution [7].

The Kuramoto model is also a one-dimensional (1D) model. However, there are some important differences between such a model and the standard RTP in one dimension. Unlike the RTP-1D model, spacial confinement in the Kuramoto system is not imposed by rigid walls but is the result of periodic boundary conditions. Also, unlike in the RTP model in one dimension, particles in the Kuramoto model are not ideal but interact with each other via a soft attractive pair potential of the form $u_{ij} \propto -\frac{K}{N}\cos(\theta_j - \theta_i)$. Because strength of interactions is rescaled by the number of particles N [24], the system is prevented from thermodynamic collapse in the limit $N \to \infty$. Such collapse is common for particles with attractive interactions but no hard-core or some other sort of divergent repulsion [25–28]. Instead of collapsing, the system undergoes phase transition from a uniform to heterogeneous distribution (from a coherent to incoherent state). The phase transition in the mean-field limit can be determined exactly.

This paper is organized as follows. In Sec. II we introduce the Kuramoto model and the extension to run-and-tumble particles. In Sec. III we consider a simple situation with both coupling parameters, K and α, set to zero. Then in Sec. IV we consider the situation $\alpha > 0$ and $K = 0$. In Sec. V we consider the complete model and analyze it using linear theory and then present numerical results. Finally, in Sec. VI we conclude the work.

II. THE KURAMOTO MODEL

The Kuramoto model is a model of synchronization stripped to a mathematical minimum [1–6]. It consists of a population of N coupled oscillators with phase θ_i and frequency ω_i distributed with a given probability $g(\omega)$. In addition, particles interact with each other so that individual frequencies are correlated. Dynamics of the model is governed by the following equation:

$$\frac{d\theta_i(t)}{dt} = \omega_i + \frac{K}{N}\sum_{j=1}^{N}\sin(\theta_j - \theta_i), \tag{1}$$

where K is the coupling strength. In the limit $N \to \infty$, the system is described exactly by the mean-field approximation. As different particles have different velocities ω_i distributed

according to $g(\omega)$, the system possesses a dynamic quenched disorder, where ω_i is the disorder variable.

A common extension of the model is to include Gaussian white noise [29],

$$\frac{d\theta_i(t)}{dt} = \omega_i + \xi_i(t) + \frac{K}{N}\sum_{j=1}^{N}\sin(\theta_j - \theta_i), \tag{2}$$

such that

$$\langle \xi_i(t)\rangle = 0, \quad \langle \xi_i(t)\xi_j(t')\rangle = 2D\delta_{ij}\delta(t-t'), \tag{3}$$

and where D is the diffusion constant.

One may construe Eq. (2) as a Langevin equation for particles moving on a circle with angular velocity ω_i and interacting with each other via a pair potential $\beta u_{ij} = -\frac{K}{D}\cos(\theta_j - \theta_i)$, where $\beta = 1/k_B T$. An advantage of this particular functional form of interactions is that it does not change when a given particle interacts with one, two, or a distribution of particles $n(\theta)$, for example, $\int d\theta' \, n(\theta)\cos(\theta - \theta_i) \propto \cos(\psi - \theta_i)$, where ψ is the center of mass of $n(\theta)$. This feature makes the model conducive to mean-field treatment.

Within the Fokker-Planck formulation, the system can be represented as

$$\frac{\partial \rho}{\partial t} = D\frac{\partial^2 \rho}{\partial \theta^2} - \frac{\partial}{\partial \theta}[\rho(\omega + Kr\sin(\psi - \theta))], \tag{4}$$

where $\rho \equiv \rho(\theta, \omega, t)$ is the normalized distribution and

$$r\sin(\psi - \theta) = \int_0^{2\pi} d\theta' \, \sin(\theta' - \theta)\int_{-\infty}^{\infty} d\omega \, g(\omega)\rho(\theta', \omega, t). \tag{5}$$

The quantity r is considered as an amplitude of an order parameter and ψ as its phase. Obviously, r is not known *a priori* but depends on a density. Equations (4),(5) represent a set of self-consistent relations.

The point where r first becomes nonzero corresponds to a phase transition. The transition is from an incoherent state, represented by a uniform distribution $\rho = 1/2\pi$ and $r = 0$, to a coherent state, represented by a heterogenous distribution and $r > 0$. The critical value of K where this occurs is determined from the following relation [assuming that $g(\omega)$ is unimodal and with even symmetry] [3–6,29]:

$$K_c = 2\left[\int_{-\infty}^{\infty} d\omega \, g(\omega)\frac{D}{D^2 + \omega^2}\right]^{-1}. \tag{6}$$

The distribution of frequencies (or angular velocities) $g(\omega)$ introduces dynamic quenched disorder, while the Gaussian white noise introduces Brownian fluctuations. For the case without quenched disorder, represented by the distribution $g(\omega) = \delta(\omega)$, the critical coupling obtained from Eq. (6) is $K_c = 2D$. On the other hand, for a system with quenched disorder but without Gaussian noise, $D = 0$, Eq. (6) evaluates to $K_c = \frac{2}{\pi g(0)}$.

One of the goals of this article is the derivation of an analogous relation to that in Eq. (6) for an extended Kuramoto model that includes run-and-tumble type of dynamics developed and analyzed in this work. The inclusion of run-and-tumble dynamics, which permits particles to sporadically change their angular velocity ω_i with a rate α, can be considered as a third source of disorder, in addition to the quenched disorder and the Gaussian noise.

Kuramoto model for self-propelled particles

As stated above, in this work we consider an extension of the Kuramoto model that incorporates self-propelled motion—or more specifically, run-and-tumble type of dynamics. While in the original model, governed by the FP equation (4), an angular velocity of an individual particle ω_i is fixed, in the extended version, individual angular velocities are allowed to evolve in time. As a consequence, every particle can sample velocities of the distribution $g(\omega)$.

On the microscopic level this means that a particle changes velocity at time intervals drawn from the Poisson distribution $\propto e^{-\alpha t}$, where α is the frequency at which this event takes place. A new velocity is then randomly drawn from the distribution $g(\omega)$. This type of dynamics corresponds to the run-and-tumble type of motion, one of the standard models of self-propelled particles [8–18]. What might be different in our version of the run-and-tumble dynamics, compared to more conventional ways it is implemented, is that the distribution of angular velocities $g(\omega)$ is arbitrary.

We note that the run-and-tumble dynamics is linked to the distribution $g(\omega)$ and, thereby, to quenched disorder of a system [7]. If a distribution is $g(\omega) = \delta(\omega)$, therefore, there is no quenched disorder, then the run-and-tumble dynamics is no longer possible, no matter what value of the parameter α. Run-and-tumble dynamics is about how fast a single particle can sample a system's quenched disorder.

The extension of the Kuramoto model just described is most conveniently incorporated within the Fokker-Planck formulation. This is done by including a linear "reaction" term to the FP equation in Eq. (4), resulting in

$$\frac{\partial \rho}{\partial t} = D\frac{\partial^2 \rho}{\partial \theta^2} - \frac{\partial}{\partial \theta}[\rho(\omega + Kr\sin(\psi - \theta))] + \alpha(\bar{\rho} - \rho), \tag{7}$$

where to simplify expressions, we introduce the average density defined as

$$\bar{\rho}(\theta, t) = \int_{-\infty}^{\infty} d\omega \, g(\omega)\rho(\theta', \omega, t). \tag{8}$$

If particles with different ω are interpreted as different species, then the "reaction" term can be viewed as a process that converts one type of particle into another.

It is impossible, based on a simple inspection of Eq. (7), to predict how the parameter α should modify Eq. (6). Both K and α act as coupling parameters, that is, they both couple different distributions $\rho(\theta, \omega, t)$ for different ω. This produces an expectation that by enhancing coupling, α should lower the critical point K_c. On the other hand, the rate α that controls the frequency with which a particle changes its angular velocity, could be regarded as a diffusion enhancing contribution, in which role it should increase the critical point K_c.

The motivation to consider such an extension of the Kuramoto model is to gain deeper and more fundamental understanding of self-propelled motion by considering it in different settings. The Kuramoto model, in particular, provides an interesting case study due to occurrence of a phase

transition. In consequence, it offers a simple setting for studying critical phenomenon with participation of self-propelled motion.

III. THE CASE $K = 0$ AND $\alpha = 0$

We start by considering a simple scenario: the Kuramoto model with both coupling parameters set to zero, $K = \alpha = 0$. Eq. (7) in this situation reduces to a diffusion-convection equation

$$\frac{\partial \rho}{\partial t} = D\frac{\partial^2 \rho}{\partial \theta^2} - \omega\frac{\partial \rho}{\partial \theta}. \tag{9}$$

For the initial distribution

$$\rho(\theta, \omega, 0) = \delta(\theta), \tag{10}$$

that is, for all particles initially placed at $\theta_i = 0$, the solution is a propagating Gaussian distribution

$$\rho(\theta, \omega, t) = \frac{e^{-(\theta-\omega t)^2/4Dt}}{\sqrt{4\pi Dt}}. \tag{11}$$

Note that the above solution ignores periodic boundary conditions, that is, $\rho(\theta + 2\pi, \omega, t) \neq \rho(\theta, \omega, t)$. As we are not interested in the distribution $\rho(\theta, t)$ *per se* but quantities derived from it, the above expression is sufficient to our purposes.

The quantity that is of interest is r defined earlier in Eq. (5). It not only measures the extent of interactions in both Eqs. (4) and (7) but also plays the role of the order parameter of a phase transition. Below, we define r a little differently from the definition in Eq. (5):

$$r(t)e^{-i\psi} = \int_{-\infty}^{\infty} d\omega\, g(\omega) \int_{-\pi}^{\pi} d\theta\, \rho(\theta, \omega, t)e^{-i\theta}. \tag{12}$$

But if we want to use the solution in Eq. (11), without periodic boundary conditions, we have to modify the above integral as

$$r(t)e^{-i\psi} = \int_{-\infty}^{\infty} d\omega\, g(\omega) \int_{-\infty}^{\infty} d\theta\, \rho(\theta, \omega, t)e^{-i\theta}. \tag{13}$$

As periodic boundary conditions are implicit in $e^{-i\theta}$, we are justified to ignore the periodicity in ρ. Substituting the solution in Eq. (11) into a modified definition for r in Eq. (13) yields

$$r(t) = e^{-Dt} \int_{-\infty}^{\infty} d\omega\, g(\omega)e^{-i\omega t}. \tag{14}$$

For r to be real valued, $g(\omega)$ ought to have an even symmetry.

The above result tells us how $r(t)$ evolves in time. At time $t = 0$, for the initial distribution in Eq. (10), $r = 1$. Without coupling between particles, there can be no phase transition and at long times $r(t) \to 0$. The above expression distinguishes between two mechanisms of relaxation: the collisional relaxation that produces exponential decay e^{-Dt}, and the collisionless relaxation that involves simple mixing as a result of quenched disorder, arising as a result of distribution of angular velocities $g(\omega)$. The collisionless mechanism depends on particular functional form of $g(\omega)$ [33].

Concrete examples

For a system without quenched disorder, represented by a singular distribution $g(\omega) = \delta(\omega)$, Eq. (14) evaluates to

$$r(t) = e^{-Dt}. \tag{15}$$

Here, the only mechanism of relaxation is collisional dissipation producing exponential decay.

Next, we consider a Lorentz distribution, $g(\omega) = \frac{1}{\pi}\frac{\omega_0}{\omega_0^2+\omega^2}$. In this case Eq. (14) evaluates to

$$r(t) = e^{-(D+\omega_0)t}. \tag{16}$$

For this type of quenched disorder, the relaxation due to collisionless mechanism is exponential, like that for collisional mechanism. The two processes are, therefore, compatible, and we can think of $D + \omega_0$ as an effective diffusion.

For a Gaussian distribution, $g(\omega) = \frac{e^{-\omega^2/2\omega_0^2}}{\sqrt{2\pi\omega_0^2}}$, Eq. (14) evaluates to

$$r(t) = e^{-Dt}e^{-\omega_0^2 t^2/2}. \tag{17}$$

Even though the collisionless and collisional relaxation have different functional form, both processes are fast.

A uniform distribution, $g(\omega) = \frac{1}{2\omega_0}$ defined on the interval $-\omega_0 \leqslant \omega \leqslant \omega_0$, is somewhat different from the two cases above. Eq. (14) for this type of quenched disorder evaluates to

$$r(t) = e^{-Dt}\frac{|\sin \omega_0 t|}{\omega_0 t}. \tag{18}$$

The collisionless relaxation in this case has a more interesting behavior; its decay is algebraic and it exhibits oscillations.

Another distribution frequently considered in the context of the Kuramoto model is a discrete binodal distribution $g(\omega) = \frac{1}{2}\delta(\omega - \omega_0) + \frac{1}{2}\delta(\omega + \omega_0)$ [30–32]. Equation (14) in this case yields

$$r(t) = e^{-Dt}|\cos(\omega_0 t)|. \tag{19}$$

For this distribution, the collisionless relaxation mechanism due to mixing does not exist. It would seem that a collisionless mechanism requires a continuous distribution $g(\omega)$.

IV. THE CASE $\alpha > 0$ AND $K = 0$

Next, we consider the Kuramoto model with run-and-tumble type of motion but without other type of interactions, $K = 0$. The FP equation describing this situation is

$$\frac{\partial \rho}{\partial t} = D\frac{\partial^2 \rho}{\partial \theta^2} - \omega\frac{\partial \rho}{\partial \theta} + \alpha(\bar{\rho} - \rho). \tag{20}$$

As we are interested in the behavior of the order parameter r, we will transform the above equation into an equivalent relation but in terms of r.

We proceed by operating on both sides of Eq. (4) with $\int_{-\pi}^{\pi} d\theta\, e^{-i\theta}$. This amounts to Fourier transforming the FP equation with respect to the wave number $k = 1$. The transformed equation is

$$\frac{\partial c_1}{\partial t} = -(D + \alpha + i\omega)c_1 + \alpha r(t)e^{-i\psi}, \tag{21}$$

where

$$c_1(\omega,t)=\int_{-\pi}^{\pi}d\theta\,\rho(\theta,\omega,t)e^{-i\theta}. \tag{22}$$

The last term in Eq. (21) comes from the definition $re^{-i\psi}=\int_{-\infty}^{\infty}d\omega\,g(\omega)c_1(\omega,t)$. If regarded as a first order inhomogeneous equation, which is possible if we ignore the fact that r is a functional of c_1, then the solution to Eq. (21) for the initial distribution in Eq. (10), can be represented as

$$c_1(\omega,t)=e^{-i\theta_0}e^{-(D+\alpha+i\omega)t}+\alpha e^{-i\psi}\int_0^t dt'\,e^{-(D+\alpha+i\omega)(t-t')}r(t'). \tag{23}$$

Finally, by operating on the above equation with $\int_{-\infty}^{\infty}d\omega\,g(\omega)$ we get

$$r(t)=R(t)+\alpha\int_0^t dt'\,r(t')R(t-t'). \tag{24}$$

The result is a convolution equation where the kernel R is given by

$$R(t)=e^{-(D+\alpha)t}\int_{-\infty}^{\infty}d\omega\,g(\omega)e^{-i\omega t}. \tag{25}$$

For $\alpha=0$, Eq. (24) recovers the result in Eq. (14). For $\alpha>0$, the evolution of $r(t)$ involves a kernel that is expected to slow down the relaxation of r.

The behavior of r, as determined by Eq. (24), depends on a particular type of quenched disorder, that is, a particular distribution $g(\omega)$. For a singular, Lorentz, discrete bimodal distribution, the equation can be solved exactly. For a uniform and Gaussian distributions exact expression doesn't seem possible, or at least it is not straightforward. For those cases, we focus on an analysis of an asymptotic behavior at long times.

A. Laplace analysis

We start by pointing out that Eq. (24) represents the Volterra integral equation of the second kind. A common method of analyzing this type of equation is by using the Laplace transform techniques. This is the approach that we are going to take.

We start by recalling the a Laplace transformed function $f(t)$ is defined as $\hat{f}(s)=\int_0^{\infty}dt\,e^{-st}f(t)$. Taking the Laplace transform of Eq. (24) yields

$$\hat{r}(s)=\frac{\hat{R}(s)}{1-\alpha\hat{R}(s)},$$

where

$$\hat{R}(s)=\int_{-\infty}^{\infty}d\omega\,\frac{g(\omega)}{s+D+\alpha+i\omega}.$$

To obtain an expression of r in real time, we use the inverse Laplace transform [34] leading to

$$r(t)=\frac{1}{2\pi i}\lim_{T\to\infty}\int_{a-iT}^{a+iT}ds\,\frac{\hat{R}(s)e^{st}}{1-\alpha\hat{R}(s)}. \tag{26}$$

The above expression has an advantage that it can be analyzed using the residue theorem that boils down to identification of the poles s_p and r can be represented in terms of residues at those poles as

$$r(t)=\sum_{s_p}\mathrm{Res}\left[\frac{\hat{R}(s)e^{st}}{1-\alpha\hat{R}(s)}\right].$$

To make the integral in Eq. (26) more intelligible, we explicitly represent $\hat{R}(s)$ of the numerator, yielding

$$r(t)=\frac{1}{2\pi i}\int_{\gamma-iT}^{\gamma+iT}\frac{ds\,e^{st}}{1-\alpha\hat{R}(s)}\int_{-\infty}^{\infty}\frac{d\omega\,g(\omega)}{s+D+\alpha+i\omega}. \tag{27}$$

The above expression allows us to distinguish two types of poles. The poles of the second fraction,

$$s_c=-D-\alpha-i\omega, \tag{28}$$

are continuous by virtue of the integral over ω. On a complex plane, those poles are represented by a line parallel to an imaginary axis and offset to the left by $-D-\alpha$.

Discrete poles of the second fractional term, on the other hand, satisfy the relation $1=\alpha\hat{R}(s_d)$, which if written explicitly leads to the following relation:

$$1=\alpha\int_{-\infty}^{\infty}d\omega\,\frac{g(\omega)}{s_d+D+\alpha+i\omega}. \tag{29}$$

Note that α appears in two different places in Eq. (38)—the fact we have already alluded to before. On the one hand, α enhances the diffusion constant D. On the other hand, it appears separately from D where it plays the role of a coupling parameter. The coupling function of α is captured by discrete poles s_d. Consequently, we restrict our analysis to s_d.

Prior to considering different concrete cases, we indicate that if $g(\omega)$ has even symmetry and is unimodal then there can be at most one pole s_d whose value is real [3,5]. For the case of a discrete bimodal $g(\omega)$, there are two poles s_d that are not restricted to a real value [31,32].

B. Concrete examples

We start with a singular distribution $g(\omega)=\delta(\omega)$—a system without quenched disorder. Equation (24) in this case is solved exactly where, unsurprisingly, it recovers the result in Eq. (15) for a system for $\alpha=0$,

$$r(t)=e^{-Dt}. \tag{30}$$

Without quenched disorder there can be no run-and-tumbling dynamics.

For a Lorentz distribution, Eq. (24) is solved exactly, leading to

$$r(t)=e^{-Dt}e^{-\omega_0 t}.$$

This is the same result as that in Eq. (16) for $\alpha=0$, implying that the run-and-tumble dynamics does not alter the evolution of $r(t)$. This is different from the case $g(\omega)=\delta(\omega)$, where the run-and-tumble dynamic simply does not exist. If we focus on a single particle trajectory (for a system with a Lorentz distribution), we would find that trajectories for different α are very different. Yet when considering dynamics collectively, by looking at the evolution of r, we detect no change. This unusual result, rather than being general is a feature of a Lorentz distribution.

To see this, we consider next a uniform distribution on the interval $-\omega_0 \leqslant \omega \leqslant \omega_0$. Because Eq. (24) cannot be solved exactly, we analyze an asymptotic behavior, $r(t) \approx e^{s_d t}$, determined by a discrete pole s_d. From the relation (29) we get

$$s_d = -(D+\alpha) + \omega_0 \cot(\omega_0/\alpha), \tag{31}$$

implying the following long time relaxation $r \propto e^{-(D+\alpha)t} e^{t\omega_0 \cot(\omega_0/\alpha)}$. Compared to evolution of r in Eq. (18) for $\alpha = 0$, we see that the run-and-tumble dynamics modifies the functional form from algebraic oscillatory to exponential monotonic.

Change of a functional form implies a discontinuity that occurs at some specific value of α, which we refer to as a point of crossover, α_{cross}. A crossover can be determined from Eq. (29) by noting that for $g(\omega)$ that is unimodal and with even symmetry s_d is real valued. This permits us to rewrite Eq. (29) as

$$1 = \alpha \int_{-\infty}^{\infty} d\omega\, g(\omega) \frac{s_d + D + \alpha}{(s_d + D + \alpha)^2 + \omega^2}. \tag{32}$$

The above integral can be interpreted as an overlap integral between two normalized distributions, $g(\omega)$ and the Lorentz distribution. Since $s_d \geqslant -D - \alpha$ (if $s_d < -D - \alpha$, the integral term becomes negative and equality cannot be satisfied), we may assume that the crossover occurs at the border value $s_d = -D - \alpha$. In such a case, the Lorentz distribution transforms into a delta function, leading to $1 = \pi \alpha_{\text{cross}} g(0)$. Consequently, we may write

$$\alpha_{\text{cross}} = \frac{1}{\pi g(0)}. \tag{33}$$

We will next establish that the coupling due to a finite α cannot produce phase transition, that is, there is no finite value of α that yields $s_d = 0$. If we take the limit $\alpha \to \infty$, Eq. (32) reduces to

$$1 \approx \frac{\alpha}{s_d + D + \alpha}. \tag{34}$$

The limiting value of s_d is $s_d = -D$ which is approached from below. This means that $s_d = 0$ can only occur if $D = 0$ and $\alpha \to \infty$. We can, therefore, exclude any phase transition. As $s_d = -D$ corresponds to a system without quenched disorder, see Eq. (30), this means that in the limit $\alpha \to \infty$ quenched disorder is completely eliminated.

Separating terms in Eq. (31) that depend on α, we may find that the contributions of a run-and-tumble motion vanish in the limit $\alpha \to \infty$, that is, $\omega_0 \cot(\omega_0/\alpha) - \alpha \to 0$. In Fig. 1 we plot Eq. (31) as a function of α.

The fact that large α eliminates a quenched disorder is not surprising to anyone familiar with propelled particles wherein the limit $\alpha \to \infty$ is considered as an equilibrium state where stationary distributions recover Boltzmann functional form [7,16].

In Fig. 2 we plot the evolution of $r(t)$ for a uniform distribution for three different values of α: below, above, and at the crossover value of α. For a uniform distribution, $\alpha_{\text{cross}} = 2\omega_0/\pi$.

For a Gaussian distribution $g(\omega)$ we get a similar behavior to that for a uniform distribution. The crossover point where

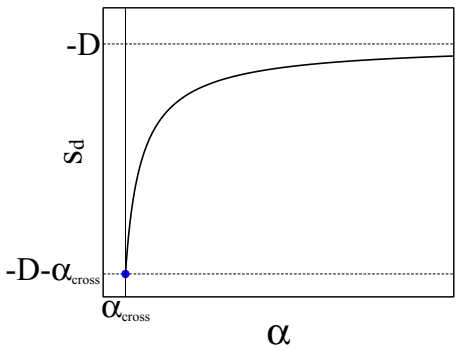

FIG. 1. Discrete pole s_d as a function of α for a uniform distribution $g(\omega)$. The results correspond to Eq. (31) for parameters $D = 1$ and $\omega_0 = 1$.

the functional form in Eq. (17) changes to an exponential decay is obtained using Eq. (33). Then as α approaches infinity, quenched disorder is eliminated.

As a last example, we consider a discrete bimodal distribution already introduced at the end of Sec. III A. Equation (24) for this distribution is solved exactly and the result is

$$r(t) = e^{-(D+\frac{\alpha}{2})t} \left| \cos(\omega_e t) + \frac{1}{2}\frac{\alpha}{\omega_e} \sin(\omega_e t) \right|,$$

where

$$\omega_e = \omega_0 \sqrt{1 - \left(\frac{\alpha}{2\omega_0}\right)^2}.$$

This is a solution for a damped oscillator. The parameter α affects the change from an underdamped to overdamped dynamics at $\alpha = 2\omega_0$.

V. FINITE K AND α

The Kuramoto model with both coupling parameters set to finite value, $\alpha > 0$ and $K > 0$, is governed by the following FP equation:

$$\frac{\partial \rho}{\partial t} = D\frac{\partial^2 \rho}{\partial \theta^2} - \omega\frac{\partial \rho}{\partial \theta} + \alpha(\bar{\rho} - \rho) - Kr\frac{\partial \rho \sin(\psi - \theta)}{\partial \theta}. \tag{35}$$

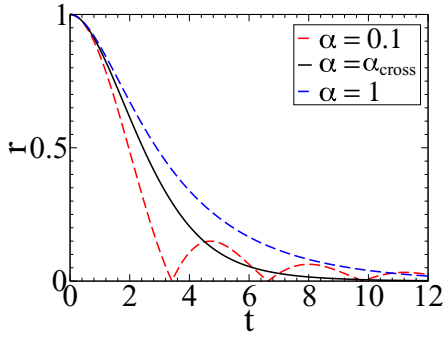

FIG. 2. Evolution of $r(t)$ for a uniform $g(\omega)$. The system parameters are $D = 0$ and $\omega_0 = 1$. The results are from dynamic simulation for $N = 10^6$ particles and time interval $dt = 0.001$ with the initial configuration corresponding to all particles placed at $\theta_i = 0$.

To apply a linear analysis of the previous section, the last term in the equation is linearized by representing the density as $\rho = \frac{1}{2\pi} + \delta\rho$, where $\delta\rho$ is the deviation from a uniform density. The linearized last term then becomes $-Kr\frac{\partial\rho\sin(\psi-\theta)}{\partial\theta} \approx \frac{K}{2\pi}r\cos(\psi-\theta)$, and the corresponding linearized FP equation is

$$\frac{\partial\rho}{\partial t} = D\frac{\partial^2\rho}{\partial\theta^2} - \omega\frac{\partial\rho}{\partial\theta} + \alpha(\bar{\rho}-\rho) + \frac{K}{2\pi}r\cos(\psi-\theta). \quad (36)$$

Following the steps in Eqs. (21) and (23) we arrive at an analogous result to that in Eq. (24):

$$r(t) = R(t) + \left(\frac{K}{2}+\alpha\right)\int_0^t dt'\, r(t')R(t-t') \quad (37)$$

with $R(t)$ is defined in Eq. (5). The equation is next transformed using the Laplace transform techniques into

$$r(t) = \frac{1}{2\pi i}\int_{\gamma-iT}^{\gamma+iT} ds\, \frac{e^{st}\hat{R}(s)}{1-(\alpha+K/2)\hat{R}(s)}, \quad (38)$$

where the discrete pole is obtained from the following relation:

$$1 = \left(\frac{K}{2}+\alpha\right)\int_{-\infty}^{\infty} d\omega\, \frac{g(\omega)}{s_d + D + \alpha + i\omega}. \quad (39)$$

The above relation can subsequently be used to obtain a critical value of K where the incoherent solution becomes unstable. Assuming that $g(\omega)$ is unimodal with even symmetry, this occurs when $s_d = 0$ leading to

$$1 = \left(\frac{K_c}{2}+\alpha\right)\int_{-\infty}^{\infty} d\omega\, g(\omega)\frac{D+\alpha}{(D+\alpha)^2+\omega^2}. \quad (40)$$

The above relation is a central result of this article. It is analogous to a similar relation for the Kuramoto model without self-consistent dynamics, see Eq. (6). It shows how the onset of self-propelled motion modifies a critical point. The parameter α appears in two places, suggesting two different roles. On the one hand, it functions as an enhancement of diffusion D. On the other hand, it enhances the coupling parameter K. The two roles work in opposite directions. Enhanced dissipation is expected to increase the critical value K_c (increased dissipation means stronger coupling is required to bring about the coherent state), while enhanced coupling is expected to reduce the critical value K_c.

A. Concrete examples

In the case of a Lorentz distribution, K_c does not depend on α, and Eq. (40) in this case leads to

$$K_c = 2(D+\omega_0).$$

Even though dynamics of individual particles is a function of α, when it comes to collective dynamics (in the case of a Lorentz distribution) no change can be detected.

For a uniform distribution $g(\omega)$, the relation in Eq. (40) yields

$$K_c = \frac{2\omega_0}{\arctan\left(\frac{\omega_0}{D+\alpha}\right)} - 2\alpha. \quad (41)$$

As the first term increases with increasing α, the second term produces an opposite trend. In the first term, α enhances diffusion, and in the second term it enhances coupling between particles. The net behavior is seen in Fig. 3 where we plot K_c in Eq. (42) as a function of α. The plot shows a monotonically decreasing K_c, indicating that the contribution of α to coupling is a dominant factor. For large α, the dependence of K_c on α is

$$\lim_{\alpha\to\infty} K_c \approx 2D + \frac{2\omega_0^2}{3}\frac{1}{\alpha},$$

where the limiting value of K_c is $2D$. As discussed in Sec. II, below Eq. (6), this value corresponds to the system without quenched disorder [when the distribution $g(\omega)$ is singular]. This once again goes to show that the self-propelled dynamics effectively leads to elimination of quenched disorder.

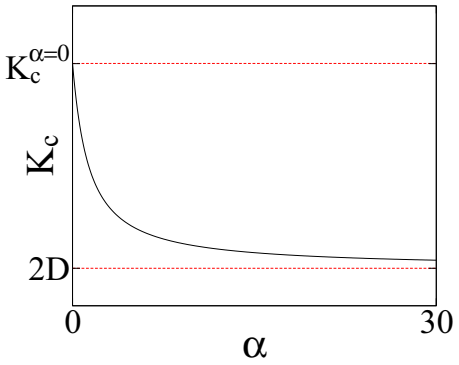

FIG. 3. K_c as a function of α as given in Eq. (42) for a uniform $g(\omega)$. The parameters are $D = 1$ and $\omega_0 = 1$.

A similar behavior is observed for a Gaussian distribution $g(\omega)$. In this case Eq. (40) evaluates to

$$K_c = \frac{2\omega_0}{\sqrt{\pi/2}}\frac{e^{-\frac{(D+\alpha)^2}{2\omega_0^2}}}{\mathrm{erfc}\left[\frac{D+\alpha}{\omega_0\sqrt{2}}\right]} - 2\alpha, \quad (42)$$

where for large α we have

$$\lim_{\alpha\to\infty} K_c \approx 2D + \frac{2\omega_0^2}{\alpha},$$

indicating a gradual elimination of quenched disorder as $K_c \to 2D$.

As a final example, we consider a discrete bimodal distribution. This scenario is more complicated, involving multiple bifurcations, full understanding of which requires nonlinear analysis [4,31,32]. Here, we limit ourselves to linear analysis and the role played by α.

From Eq. (39) we get

$$s_d = -\left(D + \frac{\alpha}{2} - \frac{K}{4}\right) \pm i\omega_0\sqrt{1-\left(\frac{2\alpha+K}{4\omega_0}\right)^2}, \quad (43)$$

indicating the existence of two poles. The result is similar to that found in Eq. (12) of Ref. [32] but limited to the case $\alpha = 0$. In the regime $4\omega_0 > K + 2\alpha$, the poles are complex. The incoherent state becomes unstable when the real part of s_d vanishes, which corresponds to

$$K_c^h = 4D + 2\alpha. \quad (44)$$

The superscript "h" designates a Hopf bifurcation and involves transformation to a time-periodic behavior of the order parameter $r(t)$. This bifurcation is shifted up as α increases. In the regime $4\omega_0 < K + 2\alpha$ where the poles are real, the phase

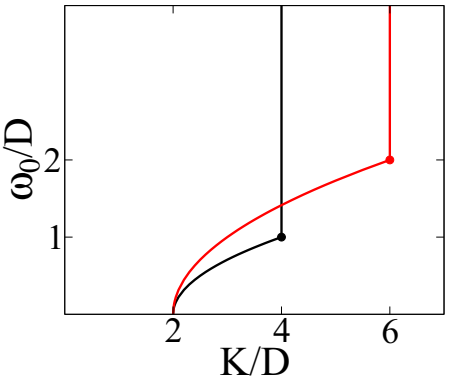

FIG. 4. Linear stability diagram for a discrete bimodal distribution $g(\omega)$ in the parameter space $(K/D, \omega_0/D)$. The incoherent state is linearly stable to the left of the lines. The black lines are for $\alpha = 0$ and red lines for $\alpha = D$. The solid circles designate a tricritical point above which the transition corresponds to a Hopf bifurcation represented by vertical lines in Eq. (44). A similar diagram for $\alpha = 0$ can be found in Fig. 1 of Ref. [32].

transition occurs when the smaller of the two poles becomes zero. This corresponds to

$$K_c = 2D + \frac{2\omega_0^2}{D+\alpha}. \tag{45}$$

In this case, K_c is shifted down with increasing α. Phase diagram constructed from Eq. (43) is shown in Fig. 4 for two cases: $\alpha = 0$ and $\alpha = D$.

B. The model for $K > K_c$

In this section we consider the Kuramoto model for a uniform distribution $g(\omega)$ for K above the critical value, $K > K_c$. In Fig. 5 we plot the data points for average value of r as a function of K obtained from dynamic simulations. The results indicate the shift of the curvatures toward lower values of K as α increases. The data points where K goes to zero agree with the theoretical prediction for K_c in Eq. (42).

A similar plot can be obtained for r plotted as a function of α with fixed K, see Fig. 6.

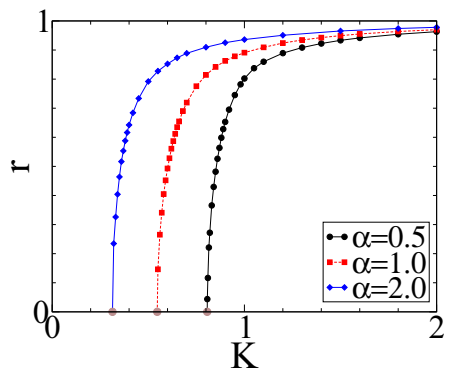

FIG. 5. Data points for an average r as a function of K for a uniform $g(\omega)$. The data points are obtained from dynamic simulations for $N = 10^5$ particles and time step $\Delta t = 0.01$. The system parameters are $\omega_0 = 1$ and $D = 0$. The three data points (brown circles) on the x axis representing K_c are from Eq. (42).

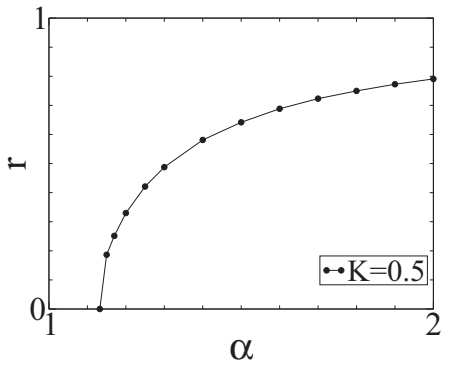

FIG. 6. Data points for an average r as a function of α for a uniform $g(\omega)$. The system parameters are $\omega_0 = 1$ and $D = 0$.

VI. CONCLUSION

In this work we extend the Kuramoto model by incorporating run-and-tumble dynamics. The extension is implemented by an addition of a linear "reaction" term in the Fokker-Planck equation. On the microscopic level, the extension allows individual particles to sample different velocities drawn from the distribution $g(\omega)$, where α is the sampling rate. The original model is recovered when $\alpha = 0$, in which case individual velocities are fixed.

How the rate of sampling α affects system dynamics depends on a particular case. For uniform and Gaussian distributions, increased α brings about reduced degree of quenched disorder and in the limit $\alpha \to \infty$ quenched disorder is completely eliminated and the system behaves as if $g(\omega) \to \delta(\omega)$. The reduction of a quenched disorder occasioned by increased α shifts down the critical value K_c.

Such a behavior, however, is not universal. In the case of a Lorentz distribution, collective dynamics, or at least the evolution of $r(t)$, is independent of α, even if the dynamics of individual particles is strongly dependent on α. Run-and-tumble dynamics for this distribution does not reduce a degree of quenched disorder. Consequently, K_c is unaffected by a sampling rate α.

For a discrete bimodal distribution, the situation is also not straightforward as there are two types of transitions from an incoherent state. One of the transitions involves Hopf bifurcation, in which case the incoherent state transforms to a state with $r(t)$ that is periodic in time. In this case, increased α shifts up the critical value of K. If the transformation to a coherent state does not involve Hopf transformation, then the behavior is similar to that for a Gaussian and uniform distributions.[1]

ACKNOWLEDGMENTS

D.F. acknowledges financial support from FONDECYT through Grant no. 1201192. D.F. would like to thank Haim Diamant for introduction to the Kuramoto model.

[1]The data that support the findings of this study are available from the corresponding author upon reasonable request.

[1] Y. Kuramoto, in *International Symposiumon Mathematical Problems in Theoretical Physics*, edited by H. Araki, Lecture Notes in Physics **39** (Springer, New York, 1975).

[2] Y. Kuramoto, *Chemical Oscillations, Waves, and Turbulence* (Springer, Berlin, 1984), pp. 68–77.

[3] S. H. Strogatz and R. E. Mirollo, Stability of incoherence in a population of coupled oscillators, J. Stat. Phys. **63**, 613 (1991).

[4] J. D. Crawford, Amplitude Expansions for instabilities in populations of globally-coupled oscillators, J. Stat. Phys. **74**, 1047 (1994).

[5] S. H. Strogatz, From Kuramoto to Crawford: Exploring the onset of synchronization in populations of coupled oscillators, Physica D **143**, 1 (2000).

[6] J. A. Acebrón, L. L. Bonilla, C. J. P. Vicente, and F. Ritort, R. Spigler, The Kuramoto model: A simple paradigm for synchronization phenomena, Rev. Mod. Phys. **77**, 137 (2005).

[7] D. Frydel, Stationary distributions of propelled particles as a system with quenched disorder, Phys. Rev. E **103**, 052603 (2021).

[8] H. C. Berg, *Random Walks in Biology* (Princeton University Press, Princeton, NJ, 1983).

[9] M. J. Schnitzer, Theory of continuum random walks and application to chemotaxis, Phys. Rev. E **48**, 2553 (1993).

[10] G. H. Weiss, Some applications of persistent random walks and the telegrapher's equation, Physica (Amsterdam) **311A**, 381 (2002).

[11] J. Tailleur and M. E. Cates, Statistical Mechanics of Interacting Run-and-Tumble Bacteria, Phys. Rev. Lett. **100**, 218103 (2008).

[12] J. Tailleur and M. E. Cates, Sedimentation, trapping, and rectification of dilute bacteria, Europhys. Lett. **86**, 60002 (2009).

[13] L. Angelani, Confined run-and-tumble swimmers in one dimension, J. Phys. A: Math. Theor. **50**, 325601 (2017).

[14] K. Malakar, V. Jemseena, A. Kundu, K. V. Kumar, S. Sabhapandit, S. N. Majumdar, S. Redner, and A. Dhar, Steady state, relaxation and first-passage properties of a run-and-tumble particle in one-dimension, J. Stat. Mech.: Theory Exp. (2018) 043215.

[15] A. Dhar, A. Kundu, S. N. Majumdar, S. Sabhapandit, and G. Schehr, Run-and-tumble particle in one-dimensional confining potentials: Steady-state, relaxation, and first-passage properties, Phys. Rev. E **99**, 032132 (2019).

[16] N. Razin, Entropy production of an active particle in a box, Phys. Rev. E **102**, 030103(R) (2020).

[17] U. Basu, S. N. Majumdar, A. Rosso, S. Sabhapandit, and G. Schehr, Exact stationary state of a run-and-tumble particle with three internal states in a harmonic trap, J. Phys. A: Math. Theor. **53**, 09LT01 (2020).

[18] I. Santra, U. Basu, S. Sabhapandit, Run-and-tumble particles in two dimensions: Marginal position distributions, Phys. Rev. E **101**, 062120 (2020).

[19] U. Erdmann, W. Ebeling, L. Schimansky-Geier, and F. Schweitzer, Brownian particles far from equilibrium, Eur. Phys. J. B **15**, 105 (2000).

[20] Y. Fily, A. Baskaran, and M. F. Hagan, Dynamics of self-propelled particles under strong confinement, Soft Matter **10**, 5609 (2014).

[21] S. C. Takatori, R. De Dier, J. Vermant, and J. F. Brady, Acoustic trapping of active matter, Nat. Commun. **7**, 10694 (2016).

[22] D. Frydel and R. Podgornik, Mean-field theory of active electrolytes: Dynamic adsorption and overscreening, Phys. Rev. E **97**, 052609 (2018).

[23] P. Sartori, E. Chiarello, G. Jayaswal, M. Pierno, G. Mistura, P. Brun, A. Tiribocchi, and E. Orlandini, Wall accumulation of bacteria with different motility patterns, Phys. Rev. E **97**, 022610 (2018).

[24] Y. Levin and R. Pakter, Comment on "Thermostatistics of Overdamped Motion of Interacting Particles", Phys. Rev. Lett. **107**, 088901 (2011).

[25] D. Frydel and Y. Levin, Soft-particle lattice gas in one dimension: One-and two-component cases, Phys. Rev. E **98**, 062123 (2018).

[26] D. Frydel, Y. Levin, Thermodynamic collapse in a lattice-gas model for a two-component system of penetrable particles, Phys. Rev. E **102**, 032101 (2020).

[27] D. Ruelle, *Statistical Mechanics: Rigorous Results* (Imperial College Press, London, 1999).

[28] M. E. Fisher and D. Ruelle, The stability of many-particle systems, J. Math. Phys. **7**, 260 (1966).

[29] H. Sakaguchi, Cooperative phenomena in coupled oscillator systems under external fields, Prog. Theor. Phys. **79**, 39 (1988).

[30] K. Okuda and Y. Kuramoto, Mutual entrainment between populations of coupled oscillators, Prog. Theor. Phys. **86**, 1159 (1991).

[31] L. L. Bonilla, J. C. Neu, and R. Spigler, Nonlinear stability of incoherence and collective synchronization in a population of coupled oscillators, J. Stat. Phys. **67**, 313 (1992).

[32] L. L. Bonilla, C. J. Pérez-Vicente, and R. Spigler, Time-periodic phases in populations of nonlinearly coupled oscillators with bimodal frequency distributions, Physica D **113**, 79 (1998).

[33] S. H. Strogatz and R. E. Mirollo, Coupled Nonlinear Oscillators Below the Synchronization Threshold: Relaxation Be Generalized Landau Damping, Phys. Rev. Lett. **68**, 2730 (1992).

[34] D. Frydel, One-dimensional Coulomb system in a sticky wall confinement: Exact results, Phys. Rev. E **100**, 042113 (2019).